

Predictive Control Method of Simulated Moving Bed Chromatographic Separation Process Based on Piecewise Affine

Song Li, Dong Wei *, Jie-Sheng Wang, Zhen Yan, and Shao-Yan Wang

Abstract—Simulated moving bed (SMB) chromatographic separation is a new type of separation technology based on traditional fixed bed adsorption operation and true moving bed (TMB) chromatographic separation technology. In order to optimize the performance of the control system, a predictive control method of SMB chromatographic separation process based on piecewise affine model is proposed. The piecewise affine modeling method was adopted to set up the SMB yield process model. The display model predictive control method is used to reduce the complexity of online operations and improve the speed of the control process. The simulation shows that the actual yield output curve of the target and impurities can fit the set target yield value. Finally, by comparing the prediction control results of the segmented affine yield model and the subspace yield model, the effectiveness of the predictive control method based on piecewise affine model is verified.

Index Terms—Simulated moving bed; Chromatographic separation; Piecewise affine; Model predictive control

I. INTRODUCTION

SIMULATED moving bed chromatographic (SMBC) separation is a new type of separation technology based on traditional fixed bed adsorption operation and true moving bed (TMB) chromatographic separation technology [1]. SMB is the main modern adsorption separation technology, which has been used in many fields, such as petrochemicals, fine chemicals, biopharmaceuticals, food processing, etc. SMBC technology is not only a frontier technology in separation science, but also a key technology for chemical separation processes. It can repeatedly use stationary phase and mobile phase to reduce costs and energy consumption, thus it is a

Manuscript received December 20, 2019; revised March 5, 2020. This work was supported by the Project by National Natural Science Foundation of China (Grant No. 21576127 and 21978123), the Basic Scientific Research Project of Institution of Higher Learning of Liaoning Province (Grant No. 2017FWDF10), and the Project by Liaoning Provincial Natural Science Foundation of China (Grant No. 20180550700).

Song Li is a postgraduate student in the School of Electronic and Information Engineering, University of Science and Technology Liaoning, Anshan, 114051, PR China (e-mail: 812738843@qq.com).

Dong Wei is with the School of Electronic and Information Engineering, University of Science and Technology Liaoning, Anshan, 114051, PR China. (Corresponding author, phone: 86-0412-5929747; e-mail: asweidong@126.com).

Jie-Sheng Wang is with the School of Electronic and Information Engineering, University of Science and Technology Liaoning, Anshan, 114051, PR China. (e-mail: wang_jiesheng@126.com).

Zhen Yan is a postgraduate student in the School of Electronic and Information Engineering, University of Science and Technology Liaoning, Anshan, 114051, PR China. (e-mail: 4139807@qq.com).

Shao-Yan Wang is a professor and master's supervisor in School of Chemical Engineering, University of Science and Technology Liaoning, Anshan, 114051, P. R. China. (e-mail: aswsy64@163.com).

green chemical technology [2].

With the development of hybrid system theory, the control discipline has entered a new research field. As the application of hybrid control theory in many research applications, many new research findings are constantly emerging. Due to the structure and type of the hybrid system is very complex, it has a variety of modeling methods. Typically, the common hybrid system modeling methods have hybrid automata (HA)[3], hybrid monitoring model[4], mixed logic dynamic (MLD)[5], linear complementarity (LC)[6], extended linear complementarity (ELC)[7], max-min-plus-scaling (MMPS) and piecewise affine system model [8-10]. According to the requirements of control system performance and modeling complexity, the corresponding hybrid system modeling method is selected. PWA model facilitates the realization of optimal control requirements and stability analysis of the controller. LC model can find the state evolution trajectory and determine the uniqueness of the trajectory. MLD model can quickly optimize hybrid systems and estimate the states of model. The above hybrid systems can realize mutual conversion between models such as positive model definiteness, bounded state variables and other additional conditions. In Ref. 11, the additional conditions of the model are given, and the conversion methods among these hybrid models are demonstrated in details.

The research and application of piecewise affine systems have attracted more and more scholars' attention. The most important reason is that the piecewise affine system is a form of expression of the hybrid system, which can facilitate the conversion between models. The piecewise affine system has a great advantage in terms of model accuracy and matching degree, which can approximate any complex nonlinear system, and accurately describe the actual complex process system. At the same time, the stability analysis of the piecewise affine system is relatively complete, which is conducive to the corresponding optimization of the system performance. A robust predictive control rule was proposed for a class of automatically switched piecewise affine systems [12]. An unstructured, non-deterministic closed-loop piecewise affine model was controlled by a multi-model linear predictive controller with constrained inputs, and the input and output stability of the control system was analyzed [13]. A method for optimizing discrete time integral sliding model control was proposed for a restricted piecewise affine system, which can ensure the stability of the closed-loop system while avoiding the controller's chattering and enhancing the robustness of the system [14]. A data driven optimization scheme for complex industrial processes was

proposed because the mechanism models of industrial process control cannot be accurately obtained [15].

Model predictive control (MPC) is an advanced optimization control algorithm composed of predictive model, rolling optimization and feedback correction. MPC method adopts the known process control models to predict future output of the model. At each control interval, the predictive control algorithm tries to optimize the future performance of the model by continuously adjusting the sequence of variables. Clarke et al. developed a controlled auto-regressive integral moving average model (CARIMA) [16]. Garic et al. proposed the internal model control (IMC) algorithm [17]. Ding Baocang et al. made a related study on the robustness of multiple time-delay systems [18]. Kayacan et al. successfully solved the trajectory tracking problem of the self-made tractor trailer system by using the fast distributed nonlinear MPC algorithm [19]. Stewart et al. designed a distributed predictive controller to satisfy the stability conditions by using a distributed implementation [20]. Farina et al. proposed a new distributed predictive control algorithm for linear discrete-time systems [21]. Markus Bambach and Michael Herty had studied to control the strain rate during the process using MPC [22]. Saeed Shamaghdari and Mohammad Haeri discuss the design of a new robust MPC algorithm for nonlinear systems [23]. The multi-variable MPC was studied based on two-point temperature control strategy [24]. An optimal control of tension and thickness for tandem cold rolling process was proposed based on receding horizon control to improve control performance and enhance the robustness of the system [25]. An extended state observer based sliding mode control of an omnidirectional mobile robot with friction compensation was studied [26].

This paper first set up the SMB yield model under the piecewise affine system, and uses the piecewise affine display predictive control method for realizing the optimal control. Then, the target yield and impurity yield are

compared with the target yield and the actual yield output of the impurity at the same target value and different target values. Finally, the actual simulation effect of the SMB chromatographic piecewise process is analyzed, and it is verified that the SMB yield model predictive control under the piecewise affine system has a good control performance.

II. SIMULATED MOVING BED CHROMATOGRAPHY SEPARATION PROCESS

The devices in the SMB chromatography separation process are composed of circulation pump, filter, constant temperature system, pressure sensor, flow rate meter, rotary valve, pipeline, control part, and a plurality of separations columns [27-28]. According to the specific requirements of the separation target compound, the number of separation columns is changed from 4 to 24, and the number of pumps is 3 to 5. The SMB system is mainly divided into the mobile phase circulation system and the stationary phase circulation system. The mobile phase circulation system make the compounds of mixed components circulate in the columns under the action of the pressure pump through the valves of the entrance port. The corresponding target separation substance is obtained at the valve outlet of extraction solution. The stationary phase circulation system simulates the flow of the stationary phase by the cooperation of two valves. The stationary phase flows in the opposite direction compared to the direction of the mobile phase.

A. Material Liquid Circulation in Chromatographic Separation Process

The chromatographic separation process is divided into different zones depending on the function, namely the solid phase regeneration zone, the two separation zones and the eluent regeneration zone. The zones of chromatographic separation process is shown in Fig. 1.

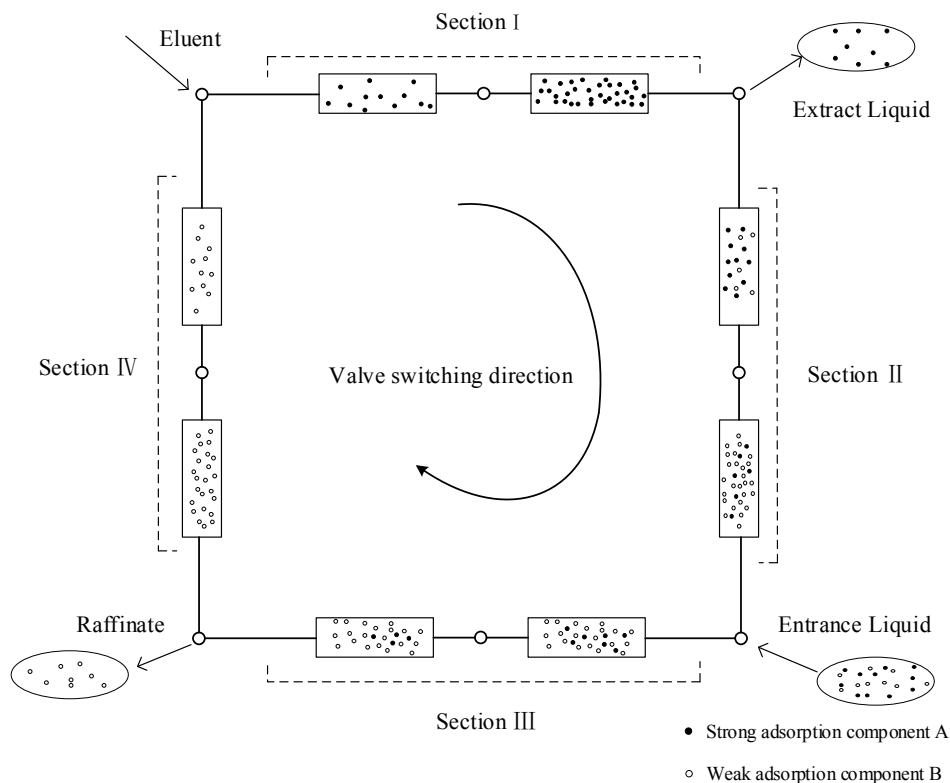


Fig. 1 Distribution map of SMB zones .

The first zone is located between the mobile phase inlet and the extract liquid outlet, the second zone is located between the extract liquid outlet and the entrance liquid inlet, the third zone is located between the entrance liquid inlet and the raffinate outlet, and the fourth zone is located between the raffinate outlet and the mobile phase inlet. In the SMB chromatography separation process, only the mobile phase in the column is circulating, and the stationary phase does not move. By controlling the valves, the position of the liquid in each zone is switched to simulate the flow of the stationary phase. The state switching of chromatographic separation is shown in Fig. 2. At the initial moment, the positions of the eluent, extract liquid, entrance liquid and raffinate are shown in the switching state 1 in Fig. 2. After t time, through the valve switching, the position of each inlet and outlet is shown in the switching state 2 in Fig. 2. After the position switching, the result is that the stationary phase forms a relative movement with the mobile phase at a speed of L/t so as to simulate the countercurrent process of the moving bed.

B. SMB structure

The core structure of the SMB device used in this paper is shown in Fig. 3. The universal SMB system is built by seven self-designed chromatographic dedicated two-way solenoid valves in each chromatographic column. There are four channels in the mobile phase inlet of each chromatographic column, which are respectively introduced into the circulating liquid of the former root column. The pumps 1, 2, and 3 are used to deliver the raw material liquid F, eluent D and eluent P. There are four pipes in the mobile phase outlet, which respectively output the current chromatographic column circulating liquid, the weak adsorption raffinate R, the strong adsorption extract liquid E, and the ordinary adsorption substance or the feedback liquid M. The seven pipes are controlled by solenoid valves. Each pipe of outlet is equipped with a detector. The microprocessor controls the working state of the solenoid valves (“on” or “off”). Under the control of the solenoid valves, the SMB system can work on multiple working modes as required.

III. PIECEWISE AFFINE SYSTEM

A. Problem Description of Piecewise Affine System

Usually, the piecewise affine system is composed of several piecewise subsystems. Because the state of the

system is different at different times, the current system state amount corresponds to the corresponding piecewise state space, and the different state subsystems belong to different piecewise subsystems according to the system state interval, so that the system state is continuously switched between different subsystems.

Given a set of mapping rules for piecewise affine system, construct a piecewise affine rule $f(x)$:

$$f(x) = \begin{cases} \theta_1, & \text{if } x \in X_1 \\ \theta_2, & \text{if } x \in X_2 \\ \vdots \\ \theta_s, & \text{if } x \in X_s \end{cases} \quad (1)$$

where, $X \subset R^n$ is a bounded polyhedron. If a specific data set $(x(k), y(k))$ is brought into a piecewise affine rule, the corresponding piecewise affine system can be expressed as:

$$y(k) = f[x(k)] + \varepsilon(k) \quad (2)$$

where, $\varepsilon(k)$ is the error of the system and satisfies the Gaussian distribution. Generally, the continuous time expression of a piecewise affine system can be described as:

$$\begin{cases} \dot{x}(t) = A_i x(t) + B_i u(t) + f_i \\ y(t) = C_i x(t) + D_i u(t) + g_i \end{cases}, \begin{bmatrix} x(t) \\ u(t) \end{bmatrix} \in \Omega_i \quad (3)$$

Similarly, the discrete time expression of the piecewise affine system can be described as:

$$\begin{cases} x(k+1) = A_i x(k) + B_i u(k) + f_i \\ y(k) = C_i x(k) + D_i u(k) + g_i \end{cases}, \begin{bmatrix} x(k) \\ u(k) \end{bmatrix} \in \Omega_i \quad (4)$$

where, $x(k) \in R^n, u(k) \in R^m, y(k) \in R^l$ is the state variable, input variable and output variable of the piecewise affine system, respectively; Ω_i is the convex polyhedron set of the system. When $\Omega_i, i=1,2,\dots$, different convex polyhedron divisions are formed. The regression model of the piecewise affine system is defined as:

$$y(k) = \varphi^T(k)\theta(v) \quad (5)$$

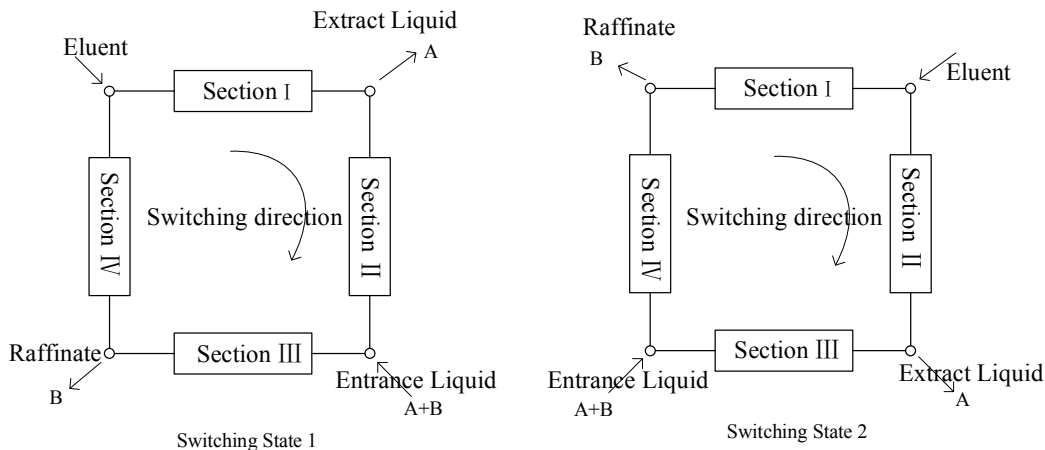


Fig. 2 Switching state schematic of SMB.

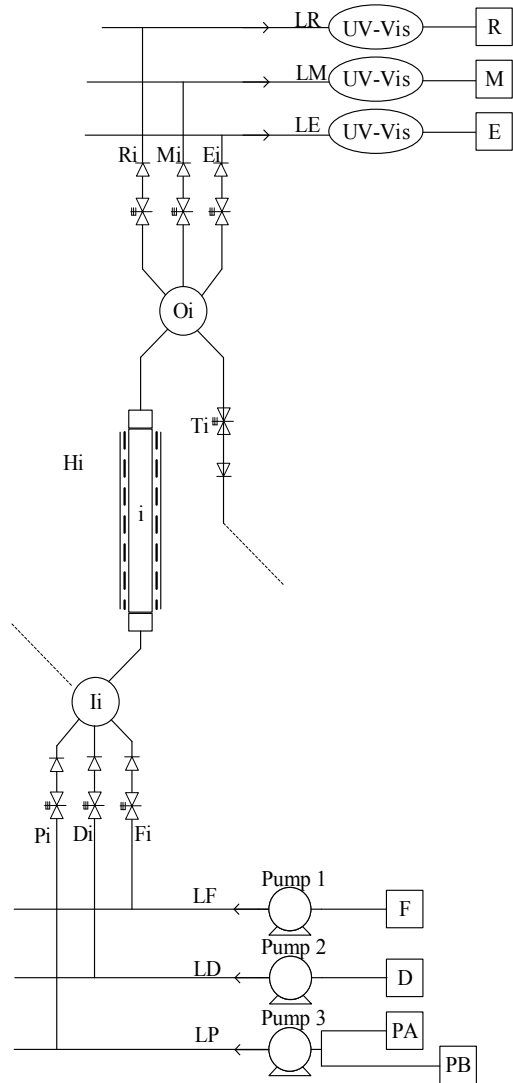


Fig. 3 SMB Chromatographic separation unit.

where, $v \in \{1, 2, \dots, s\}$ represents different piecewise models, s represents the number of piecewise models, θ_i is the system parameter of the affine subsystem. $\varphi(k)$ is the regression vector, that is to say:

$$\varphi(k) = [y(k-1), \dots, y(k-n_a), u(k-1), \dots, u(k-n_b), 1]^T \quad (6)$$

The state vector $x(k)$ can be described as:

$$x(k) = [y(k-1), \dots, y(k-n_a), u(k-1), \dots, u(k-n_b)]^T \quad (7)$$

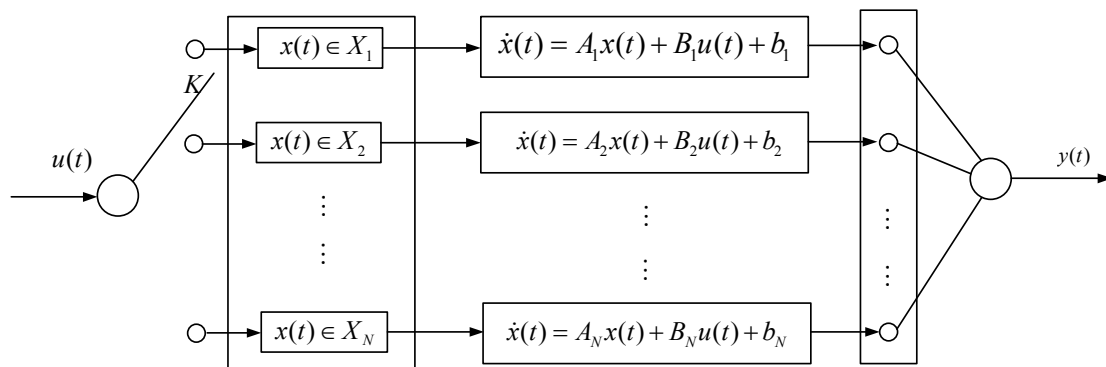


Fig. 4 Piecewise affine system structure.

where, $y(k) \in \mathbb{R}^l$.

The piecewise affine system is a system switching strategy composed of several system state space regions. Each state region corresponds to a corresponding state space model. The switch is used to determine the state space region corresponding to the system input. Assume that the piecewise affine system is composed of piecewise subsystems of 1, 2, ..., N, a complete piecewise affine system is constructed according to the corresponding switching law. The structure diagram of the piecewise affine system is shown in Fig.4.

The piecewise affine system has the characteristic attribute of model switching, and it depends on the change of system state. When the system state belongs to a certain state space region, the process system model is described as a local system identification model in this space region. At some point, when the system state changes, the current system state belongs to another state space region, the identification model of the process system changes to a local system identification model in the new state space domain.

The difference between a continuous piecewise affine system and a discrete piecewise affine system is whether its system state trajectory is continuous on the boundary of the state space domain. The continuous piecewise affine systems are continuous on the boundary of the state space domain. However, the discrete piecewise affine systems are not continuous on the boundary of the state space domain. Therefore, the continuous piecewise affine systems switch between local system identification models in different state space domains, and it can only switch correspondingly in adjacent state space domains. Compared with the continuous piecewise affine system, because the discrete state trajectory of the discrete piecewise affine system is not continuous, the local system identification model of the discrete piecewise affine system can be switched in the global state space domain.

B. State Change Track of Piecewise Affine System

Since the piecewise affine system relies on the state space area corresponding to the current moment state of the system to perform the corresponding switching operation, the system state change trajectory is an intuitive description of the state of the piecewise affine system. In order to obtain the state trajectory of the piecewise affine system, the initial state of the system is given first, then it is brought into the PWA system model so as to obtain the value of the updated system state variable.

Through repeated iterative updates, finally obtain the state trajectory of the PWA system. Fig. 5 shows the state change trajectory of state x_1 and state x_2 under the piecewise affine system.

IV. MODELING METHOD OF PIECEWISE AFFINE SYSTEM

A. Equilibrium Point of Piecewise Affine System

In the modeling process of a nonlinear complex system, the equilibrium points of the system may be some independent and scattered points. The specific solution steps are described as follows.

- (1) Given the input variable as a constant u_{eq} .
- (2) Solve $f(x_{eq}, u_{eq}) = 0$ to obtain the state of the system x_{eq} .
- (3) Specify the interval range and repeat the process so as to verify that $x_{eq} \in X_i$ holds.

Solving the equilibrium points of the piecewise affine system can provide the prerequisites for the subsequent division of the state space region of the piecewise affine system. The corresponding spatial tangent planes can be easily found by using the system equilibrium points.

B. Division of State Space Region of Piecewise Affine System

With the help of the equilibrium points of the piecewise affine system, the space near the system equilibrium points can be approximated to construct a space tangent plane, and the state space can be divided into different state space regions through the space tangent plane. The different space regions divided by the tangent plane form the state space region under the independent action of the piecewise subsystem model. Several state space regions are obtained after the division of the space state region, and each state space region is a hypersurface surrounded by a finite number of half-planes. The finite number of half-planes can be described by the following inequalities.

$$(c_{i,j})^T x + d_{i,j} \geq 0 \tag{8}$$

The division of the state space region is to describe each divided state subspace region as a vector inequality, that is:

$$C_i x + D_i \geq 0, x \in X_i \tag{9}$$

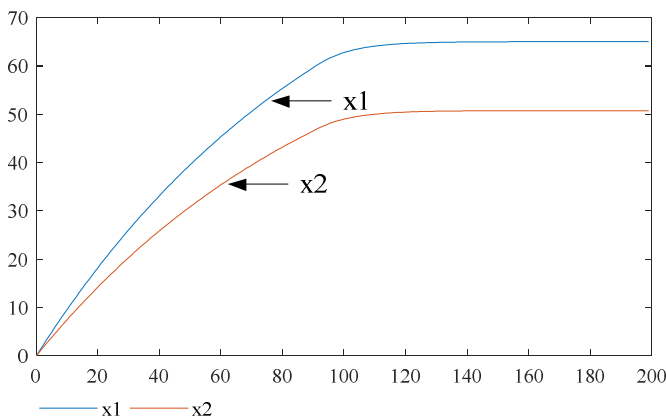


Fig. 5 State change track of PWA.

where, $C_i \in R^{p \times n}, D_i \in R^p$. When the division of the state space area occurs at the boundary position, it can be described as:

$$\begin{aligned} x &\in X_i \cap X_j, i, j \in I, \\ C_i x + D_i &= C_j x + D_j \end{aligned} \tag{10}$$

The division of the state space region is shown in Fig. 6. If the system state domain X_i directly enters the system state domain X_j and does not pass through any other state regions during the state transition, that is to say $i, j \in I, i \neq j, X_j$ is the immediate neighborhood of X_i . If the system state is terminated after reaching the system state domain X_i , the system state domain X_i is the termination domain of the system. When the system state domain X_i is convex, then:

$$X_i = \{x | G_i x + g_i \geq 0\} \tag{11}$$

Similarly, when the division of the system state domain occurs at the boundary position, obtain:

$$G_i x + g_i = G_j x + g_j, x \in X_i \cap X_j \tag{12}$$

Any nonlinear system can be described by a piecewise affine system. Specifically, the state space is divided into several regions, and the corresponding subsystem models are constructed for the subsystems in each region. The constructed subsystem model can fully meet the process output of any state in the current area. In actual process control, according to the current state of the system corresponding to the corresponding area of the piecewise affine system, the piecewise subsystem related to this area can be located. After that, the model under the piecewise subsystem is controlled. The mathematical expression for the division of the system's state domain is a matrix linear inequality, which can be solved with the help of corresponding solving tools, such as the LMI toolbox.

C. Representation of State Space Region Division of Piecewise Affine System

(1) Ellipse Set Representation

The partitioned area of the PWA system is represented as an ellipse set so as to effectively reduce the complexity of variables. Meanwhile it is more suitable for the calculation of matrix inequality.

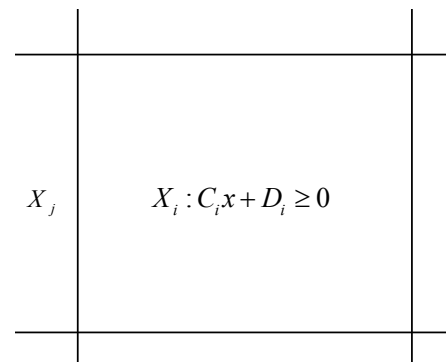


Fig. 6 Division of state space regions.

Therefore, when the differential equation is used as the system model, the representation form of the ellipse set is often used as the area division of the PWA system. For the elliptic set form, there is $X_i \subseteq \varepsilon_i$, where ε_i is the elliptic set. Then:

$$\varepsilon_i = \{x \mid \|E_i x + e_i\| \leq 1\} \tag{13}$$

The matrix inequality has the following form:

$$\begin{bmatrix} x \\ 1 \end{bmatrix}^T \begin{bmatrix} E_i^T & * \\ e_i^T & -1 + e_i^T e_i \end{bmatrix} \begin{bmatrix} x \\ 1 \end{bmatrix} \leq 0 \tag{14}$$

When $X_i = \{x \mid d_1 < c_i^T < d_2\}$ (state boundary d_1, d_2 are constants), the coefficients of the ellipse set are calculated by:

$$\begin{cases} E_i = \frac{2c_i^T}{d_2 - d_1} \\ e_i = -\frac{d_2 + d_1}{d_2 - d_1} \end{cases} \tag{15}$$

(2) Convex Polyhedron Representation

The division of the piecewise affine system can also be expressed in the form of a convex polyhedron. Compared with elliptic set, convex polyhedron is more suitable for complex hybrid model to express the piecewise control strategy under complex control system intuitively. In order to explain the division of the state space region of the piecewise affine system in details, the state space division of the dual integrator model is described below. The dual integrator

model can be described as $y(t) = u(t) / s^2$. The corresponding polyhedron partition and state change trajectory are shown in Fig. 7. The entire plane in the Fig. 7 is the state space plane of the dual integrator system. The entire state space plane is divided into 7 different state space planes by the balance point boundary. For convenience of observation, the divided space state regions are represented by different colors. The curve in the Fig. 7 is the state change track of the dual integrator system state switching in different state space regions.

V. MODEL PREDICTIVE CONTROL ALGORITHM BASED ON PIECEWISE AFFINE

The model predictive control uses a rolling time domain optimization method based on the state of the system sampling time to solve the optimal control amount of the current time online, and apply it to the input of the next time. The conventional MPC algorithm repeatedly calculates the optimal control amount at each sampling time, and applies it to the system to achieve the optimal control. This control method can correct the control error in the next time while the system is robust. However, the conventional MPC method must perform the corresponding calculations before each control action is applied, which will cause delays and lags in the actual process control. Therefore, in order to solve the problem of control lag in the conventional MPC, a display MPC can be adopted. The display MPC method consists of offline calculation and online calculation. The core implementation method is to split the system's optimization control index, apply the multi-parameter optimization method, and make the calculation of the control law offline in advance, thereby the calculation amount of the online calculation part is reduced, and the control efficiency of the system is improved.

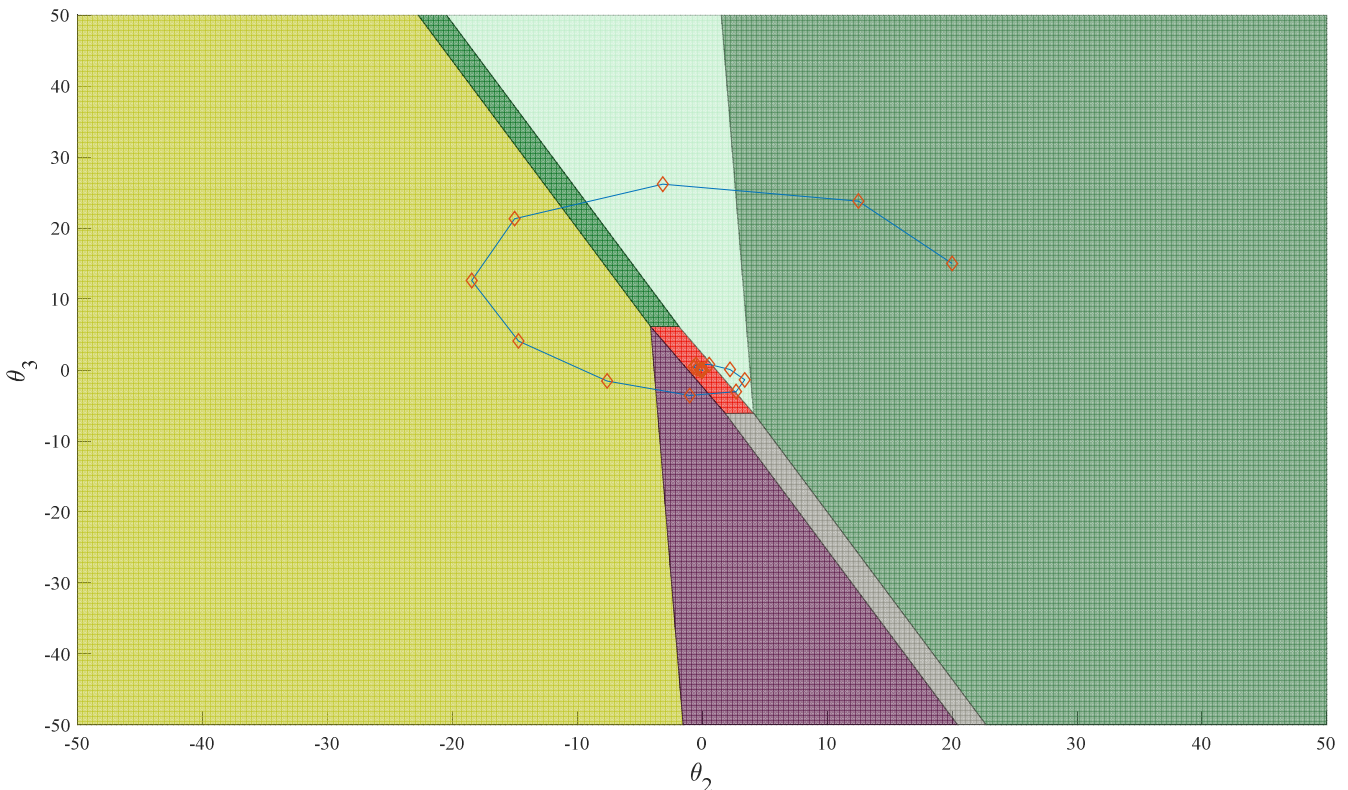


Fig. 7 Polyhedral state space partition and state change trajectory.

Suppose the PWA system is described as follows.

$$\begin{aligned} x(k+1) &= f_{PWA}(x(k), u(k)) + f_i \\ &= A_i x(k) + B_i u(k) + f_i \\ y(k) &= C_i x(k) + D_i u(k) + g_i \end{aligned} \quad (16)$$

where, $\begin{bmatrix} x(k) \\ u(k) \end{bmatrix} \in \Omega_i$, $\{\Omega_i\}_{i=1}^s \stackrel{\Delta}{=} \left\{ \begin{bmatrix} x \\ u \end{bmatrix} : H_{ix} x + H_{iu} u \leq K_i \right\}$, $i = 1, 2, \dots, s$.

It is a polyhedron set divided between the system state and the system input; $u(k) \in R^m, x(k) \in R^n$ are the input and state variables of the system; A_i, B_i, b_i are the system matrix, input matrix, and piecewise affine vector of the i -th piecewise subsystem. The switching neighborhood of subsystem i and subsystem j can be represented by the symbol X_{ij} , that is to say:

$$X_{ij} = \{x(k) \in R^n \mid \exists k \geq 0, x(k) \in X_i, x(k+1) \in X_j, i, j \in I\} \quad (17)$$

The predictive control method for PWA system is a combination of MPC algorithm and multi-parameter programming. In the offline state, the system's control law is first obtained, which reduces the complexity of online update calculations, improves the decision-making efficiency of the control system, and makes it more practical.

(1) Offline Calculation

The optimized performance indicator is defined as:

$$\begin{aligned} J_N^*(x(0)) &= \min_{U_0^{N-1}} J(U_0^{N-1}, x(0)) \\ &= \min_{U_0^{N-1}} \{ \|Q_N(x(N) - x_r)\|_\infty + \\ &\quad \sum_{k=0}^{N-1} \|R(u(k) - u_r)\|_\infty + \|Q(x(k) - x_r)\|_\infty \} \end{aligned} \quad (18)$$

Subject to:

$$\begin{cases} x(k+1) = A_i x(k) + B_i u(k) + f_i \\ x(N) \in T_{set} \end{cases} \quad (19)$$

And satisfies:

$$\begin{bmatrix} x(k) \\ u(k) \end{bmatrix} \in \Omega_i, i = 1, 2, \dots, s. \quad (20)$$

where, $U_0^{N-1} \stackrel{\Delta}{=} [u(0)^T, u(1)^T, \dots, u(N-1)^T] \in R^n$ is the control vector, N is the control time domain, T_{set} is the terminal constraint set, Q_N, Q, R is a weight matrix and satisfies the column full rank. By using the multi-parameter and dynamic linear programming theory, the above optimized system performance indicator can be transformed into:

$$\begin{aligned} J_j^*(x(j)) &= \min_{u(j)} \{ \|R(u(j) - u_r)\|_\infty + \\ &\quad \|Q(x(j) - x_r)\|_\infty + J_{j+1}^*(x(j+1)) \} \end{aligned} \quad (21)$$

Subject to:

$$\begin{cases} x(j+1) = f_{PWA}(x(j), u(j)) \\ x(j+1) \in T_{j+1} \end{cases} \quad (22)$$

This control law is an explicit control law, and the system input has a linear relationship with the system state. It can convert online calculations to offline calculations in advance. In the process of online calculation, the corresponding control amount can be obtained by simply comparing the state of the online calculation with the state in the explicit control law obtained from the previous offline calculation and simple linear solution.

(2) Online Calculation

The principle of online calculation is that the state of the system at the current moment is based on the segmentation affine rule of the control law, then through a series of calculations, the corresponding output of the system in this state can be obtained. It can be known from the principle of online calculation that it is a series of state mapping processes corresponding to a series of state points. The method often used for this process is the sequential search method. For explicit controllers, a sequential search method is used to sequentially find the corresponding one by one in accordance with the order of partition 1, partition 2, ... and determine whether the state belongs to the range of the partition until the partition corresponding to the state is found and terminated. The flowchart of online calculation process is shown in Fig. 8. Generally, if the display controller contains N different status partitions. The i -th state partition can be recorded as $P_i = \{x \mid H_i x \leq K_i\}$, where n_{R_i} represent the number of hyperplanes in the partition. The steps for online calculation are described as follows.

Step 1: Save the current state $x(k)$ of the system.

Step 2: Let $i = 1$.

Step 3: Corresponding to partition i , judge whether $H_i x \leq K_i$ is satisfied or not. If this condition is satisfied, $x(k) \in P_i$ and go to Step 5, otherwise go to Step 4.

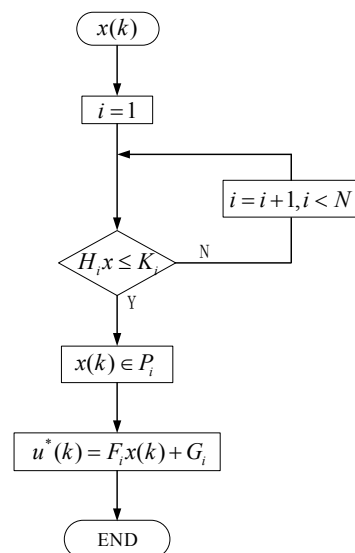


Fig. 8 The flowchart of online process calculation.

Step 4: $i = i + 1, i < N$. Go to Step 3.

Step 5: Substitute $x(k)$ into the control law $u^*(k) = F_i x(k) + G_i$, and calculate the corresponding output.

Step 6: End.

VI. SIMULATION EXPERIMENTS AND RESULT ANALYSIS

A. State Space Model Based on Piecewise Affine System

(1) Select Input and Output Variables

This paper collected the actual operating data of a SMB chromatography separation device. The number of data is 1400 groups, which has target substance purity, impurity purity, target substance yield, impurity yield, and switching time. The input-output data are listed in Table 1. The model input vector and output vector are $U=(u_1, u_2, u_3)$ and $Y=(y_1, y_2)$, where, u_1, u_2, u_3 are F pump flow rate, D pump flow rate and switching time, y_1 is the target substance yield, and y_2 is the impurity yield.

(2) State Space Model of Chromatographic Separation System

The piecewise affine modeling method is adopted to model the SMB yield process system. The scopes of the four segmented subsystems are $X_1 \in [0, 0.4]$, $X_2 \in [0.4, 0.6]$, $X_3 \in [0.6, 0.8]$ and $X_4 \in [0.8, 1.0]$. The SMB yield model based on the piecewise affine system can be calculated as:

$$\begin{cases} x(k+1) = \begin{bmatrix} 2.44 & -1.383 & 0.805 & -0.295 \\ 2 & 0 & 0 & 0 \\ 0 & 1 & 0 & 0 \\ 0 & 0 & 0.5 & 0 \end{bmatrix} x(k) + \begin{bmatrix} 4 \\ 0 \\ 0 \\ 0 \end{bmatrix} u(k) \\ y(k) = [1.334 \quad -1.154 \quad 2.038 \quad -2.647]x(k) + 0.7706u(k) \\ x \in X_1 \end{cases} \quad (23)$$

$$\begin{cases} x(k+1) = \begin{bmatrix} 2.44 & -1.383 & 0.805 & -0.295 \\ 2 & 0 & 0 & 0 \\ 0 & 1 & 0 & 0 \\ 0 & 0 & 0.5 & 0 \end{bmatrix} x(k) + \begin{bmatrix} 4 \\ 0 \\ 0 \\ 0 \end{bmatrix} u(k) \\ y(k) = [0.893 \quad -0.758 \quad 1.475 \quad -2.05]x(k) - 3.757u(k) \\ x \in X_2 \end{cases} \quad (24)$$

$$\begin{cases} x(k+1) = \begin{bmatrix} 2.44 & -1.383 & 0.805 & -0.295 \\ 2 & 0 & 0 & 0 \\ 0 & 1 & 0 & 0 \\ 0 & 0 & 0.5 & 0 \end{bmatrix} x(k) + \begin{bmatrix} 0.25 \\ 0 \\ 0 \\ 0 \end{bmatrix} u(k) \\ y(k) = [0.139 \quad -0.112 \quad 0.096 \quad -0.098]x(k) - 0.019u(k) \\ x \in X_3 \end{cases} \quad (25)$$

$$\begin{cases} x(k+1) = \begin{bmatrix} 2.44 & -1.383 & 0.805 & -0.295 \\ 2 & 0 & 0 & 0 \\ 0 & 1 & 0 & 0 \\ 0 & 0 & 0.5 & 0 \end{bmatrix} x(k) + \begin{bmatrix} 0.25 \\ 0 \\ 0 \\ 0 \end{bmatrix} u(k) \\ y(k) = [0.111 \quad -0.09 \quad 0.076 \quad -0.078]x(k) - 0.0035u(k) \\ x \in X_4 \end{cases} \quad (26)$$

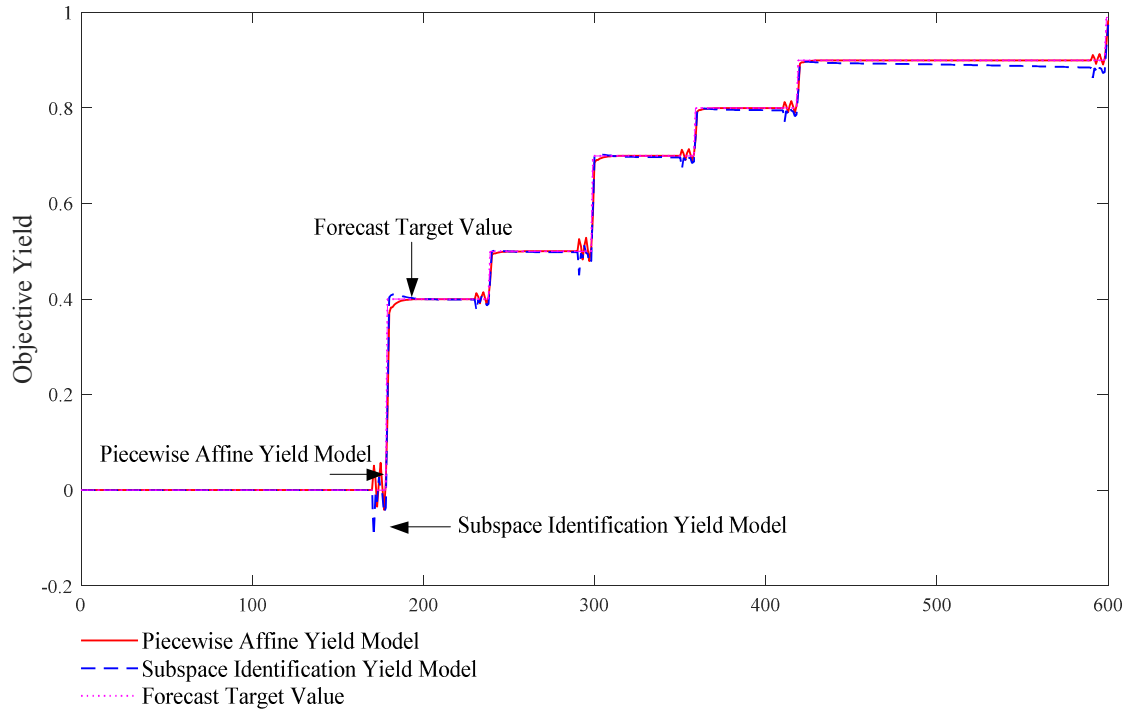
B. Yield Model Predictive Control

Set the prediction range is 600, the model control time domain is 10, and the prediction time domain is 20. The actual process data is used as the reference experience value, and the target yield is set to 5 yield region segments: $[0, 0.4]$, $[0.4, 0.5]$, $[0.5, 0.7]$, $[0.7, 0.8]$, $[0.8, 0.9]$, and $[0.9, 0.99]$. Within the range of a given yield region, the subspace yield model and the piecewise affine yield model are respectively subjected to predictive control, and the output prediction curves of each yield model are obtained, as shown in Fig. 9 (a)-(b).

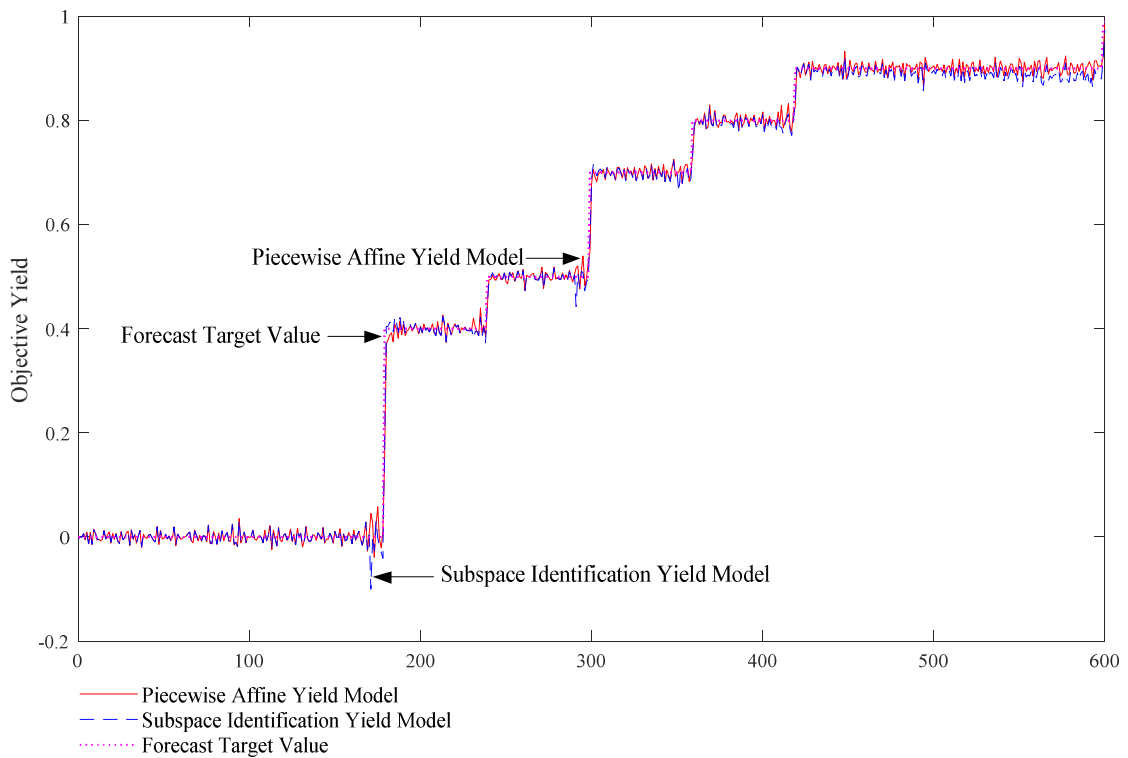
It can be seen from the yield prediction curves under the piecewise affine and subspace identification yield model system that the yield output curve of the piecewise affine system can completely fit the output target value of the target yield, and can smoothly transition to the corresponding yield gradient. In the case of noise fluctuation, although the piecewise affine yield model makes the yield output fluctuate up and down under noise interference, the fluctuation range can be controlled near the target value and the fluctuation range is smaller. Although the subspace yield prediction curve has good control and output effects, compared with the yield output curve of the piecewise affine yield model, it will produce larger deviations and fluctuations. Therefore, the piecewise affine yield model has better model matching and control performance than the subspace yield model.

TABLE 1 INPUT-OUTPUT DATA SETS

F pump flow rate	D pump flow rate	Switching time	Target substance purity	Impurity purity	Target substance yield	Impurity yield
0.10	0.50	11.00	0.16	0.18	0.05	0.43
0.10	0.50	12.00	0.75	0.32	0.23	0.84
0.10	0.50	13.00	0.96	0.41	0.42	0.96
...
0.49	1.99	18.00	1.00	0.33	0	1.00
0.49	1.99	19.00	1.00	0.33	0	1.00
0.49	1.99	20.00	1.00	0.33	0	1.00



(a) Yield model prediction curve without noise.



(b) Yield model prediction curve with noise.

Fig. 9 Yield model prediction curves.

Two sets of square wave signals under different parameters are given in two groups (groups A and B), that is to say the square wave width is 60, the square wave amplitude range is [0.1,0.6], and the square wave width is 50, and the square wave amplitude range is [0,0.95]. Within a given area, the piecewise affine yield model and the subspace yield model are used for model predictive control, and the output prediction curves of each yield model under different inputs are obtained by the MPC algorithm. The simulation results are shown in Fig. 10 (a)-(d).

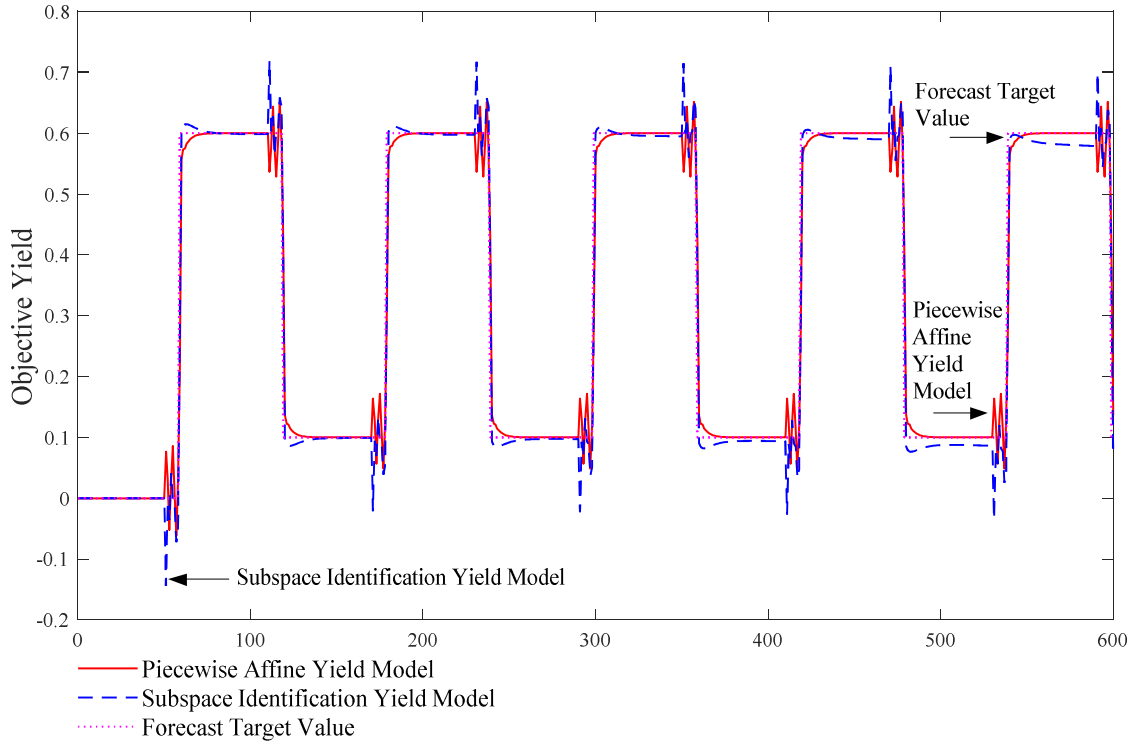
It can be known from the above simulation results that

when two sets of different square wave signals are given under noise-free conditions, the target yield curve of the piecewise affine yield model can rise to the highest value or fall to the lowest value of the square wave, the transition smoothly to the target value of the yield output. At the inflection points to the right of the lowest and highest values of the square wave, the actual yield will have a short-term shock. The target yield curve of the subspace yield model has a significant overshoot during the square wave rising to the highest value or falling to the lowest value. Compared with the piecewise affine yield model, the yield curve has a large

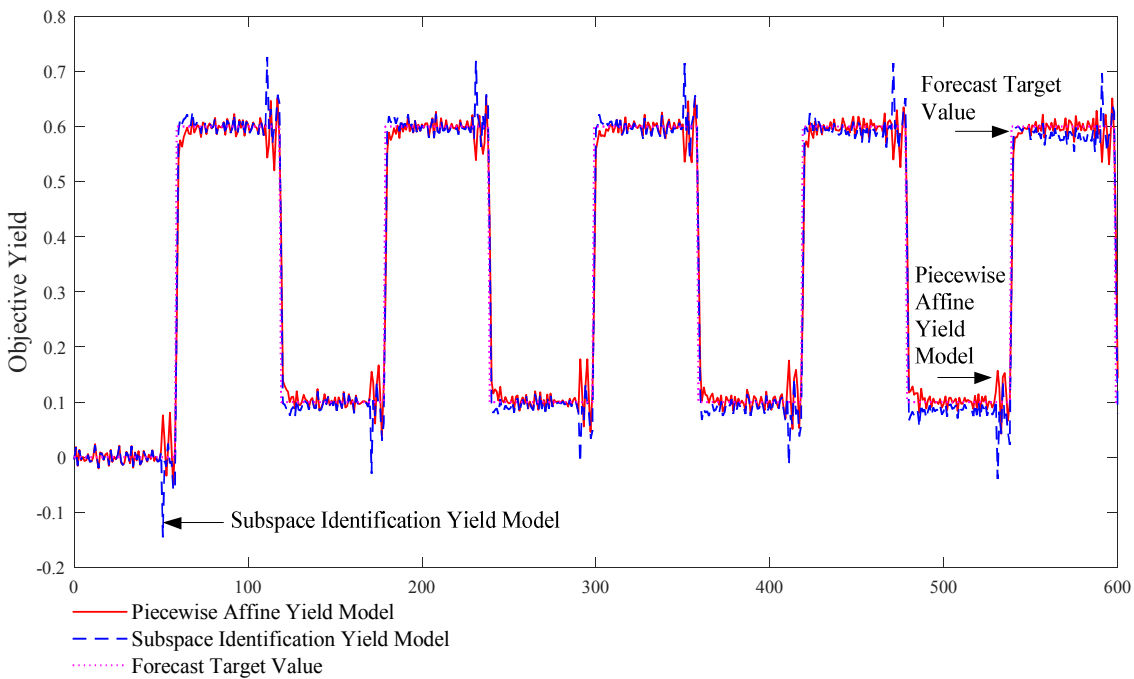
overshoot. When the inflection points to the right of the minimum and maximum values of the square wave are reached, the subspace yield curve will produce greater oscillations than the piecewise affine yield curve.

Given two different sets of square wave signals under noise conditions and compared with the target yield curve of the subspace yield model, the target yield curve of the segmented affine yield model still has smaller oscillation amplitude and better anti-disturbance performance. Although, at the inflection points of each phase of the square wave, the

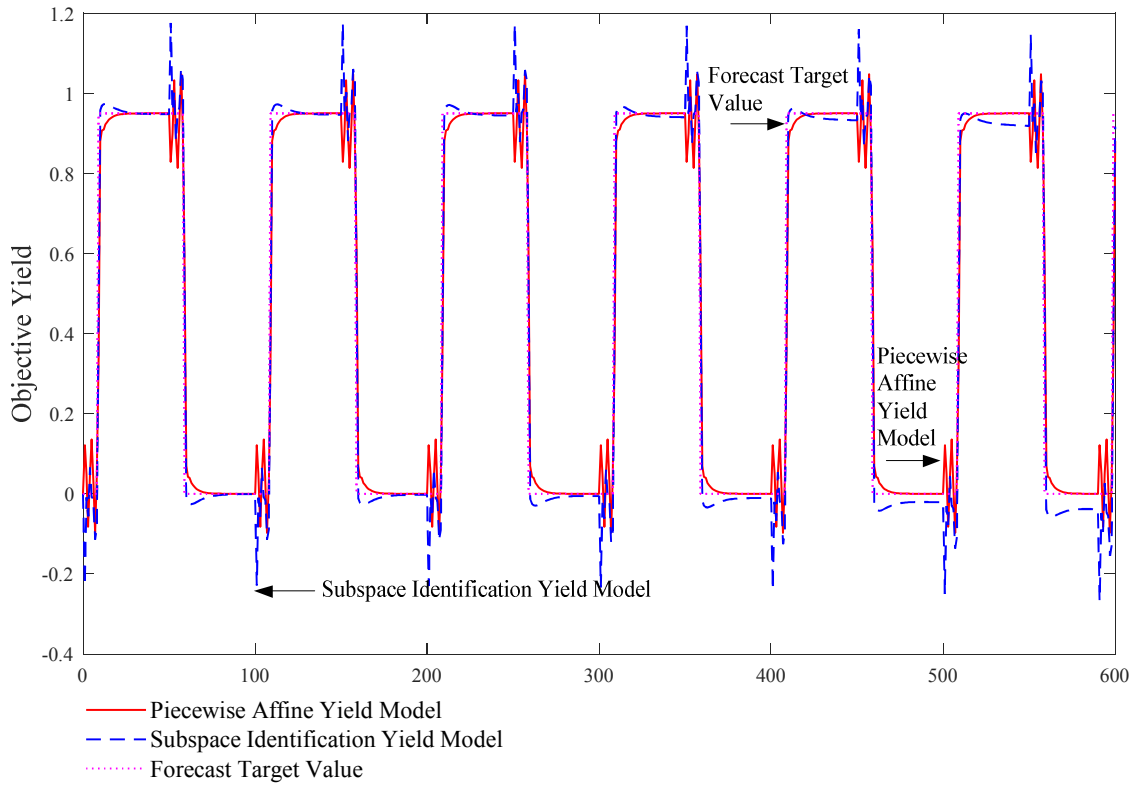
two models cannot completely fit the ideal square wave yield output curve. The main reason is that due to the inevitable measurement errors in the data sampling, the fitting output error of the model is eventually caused. However, the errors are controlled within an acceptable range, and the true value of the yield at each stage can still be fully fitted to the given target output value. The final simulation results show that the degree of fitting of the yield output of the SMB piecewise affine yield model is better than that of the SMB subspace yield model.



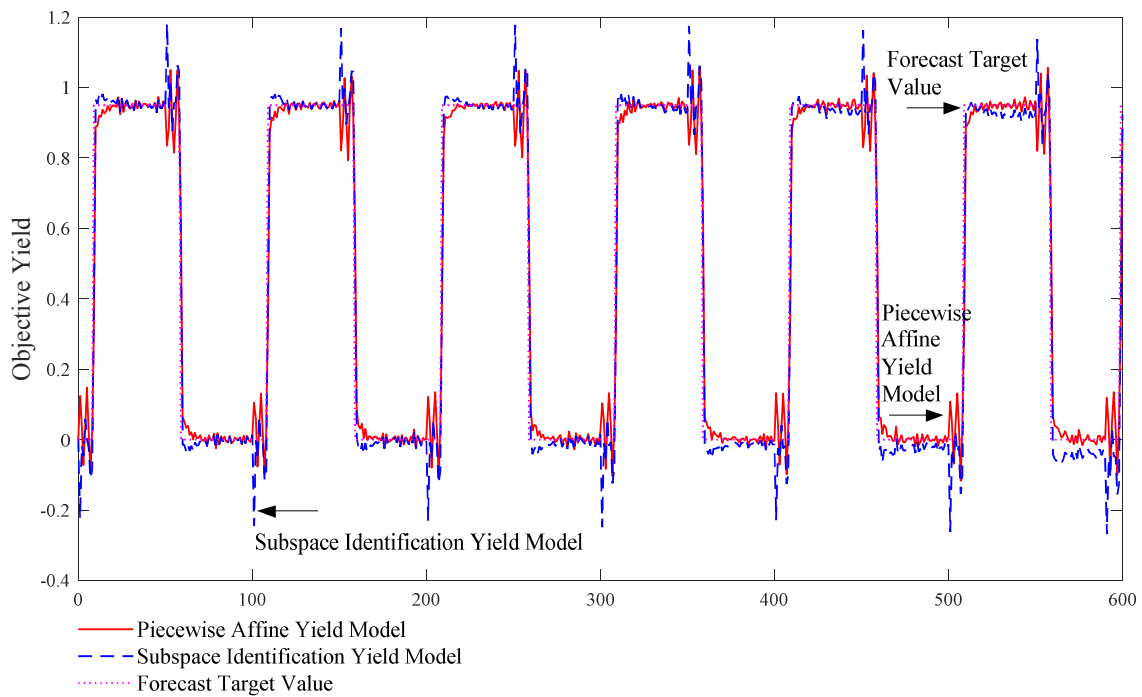
(a) The yield model prediction curve without noise of Group A square wave signal.



(b) The yield model prediction curve with noise of Group A square wave signal.



(c) The yield model prediction curve without noise of Group B square wave signal.



(d) The yield model prediction curve with noise of Group B square wave signal.

Fig. 10 The yield model prediction curve of square wave signal.

VII. CONCLUSION

In this paper, a piecewise affine model of the SMB yield process system is obtained based on the piecewise affine modeling method. To optimize the performance of the control system, a predictive control of the SMB chromatographic separation yield model based on the piecewise affine system is proposed. The display MPC method is used to reduce the complexity of online operations and improve the control speed. In the simulation experiments,

the output of the target yield is compared in different yield zones, and the output follow-up of the target yield under different square wave output signals are set. The experiment results show that compared with the subspace yield model, the actual yield output curve of the predictive control system based on the piecewise affine model can better fit the set target yield value. The feasibility and superiority of the MPC method of the piecewise affine model is verified by simulation experiments.

REFERENCES

- [1] Püttmann, Andreas, S. Schnittert, U. Naumann, and E. Von Lieres, "Fast and Accurate Parameter Sensitivities for the General Rate Model of Column Liquid Chromatography," *Computers & Chemical Engineering*, vol. 56, pp. 46-57, 2013.
- [2] S. Qamar, J. Nawaz Abbasi, S. Javeed, and A. Seidel-Morgenstern, "Analytical Solutions and Moment Analysis of General Rate Model for Linear Liquid Chromatography," *Chemical Engineering Science*, vol. 107, pp. 192-205, 2014.
- [3] Y. L. Shang, D. H. Hou, and F. Z. Gao, "Finite-time Output Feedback Stabilization for a Class of Uncertain High Order Nonholonomic Systems," *Engineering Letters*, vol. 25, no. 1, pp. 39-45, 2017.
- [4] J. Lunze, B. Nixdorf, and H. Richter, "Process Supervision by Means of Hybrid Model," *Journal of Process Control*, vol. 11, no. 1, pp. 89-104, 2001.
- [5] A. Benporad, and M. Morari, "Control of Systems Integrating Logic, Dynamics, and constraints," *Automatica*, vol. 35, no. 3, pp. 407-427, 1999.
- [6] J. L. Shen, and J. S. Pang, "Linear Complementarity Systems: Zeno States," *SIAM Journal on Control and Optimization*, vol. 44, no. 3, pp. 1040-1066, 2006.
- [7] M. S. Gowda, "On the Extended Linear Complementarity Problem," *Mathematical Programming*, vol. 72, no. 1, pp. 33-50, 1996.
- [8] M. Johansson, and A. Rantzer, "Piecewise Linear Quadratic Optimal Control," *IEEE Transactions on Automatic Control*, vol. 45, no. 4, pp. 629-637, 2000.
- [9] A. Benporad, G. Ferrari-Trecate, and M. Morari, "Observability and Controllability of Piecewise Affine and Hybrid systems," *IEEE Transactions on Automatic Control*, vol. 45, no. 10, pp. 1864-1876, 2000.
- [10] L. L. Wang, "Dynamic Output Feedback Guaranteed Cost Control for Linear Nominal Impulsive Systems," *Engineering Letters*, vol. 26, no. 4, pp. 405-409, 2018.
- [11] W. P. M. H. Heemels, B. De Schutter, and A. Bemporad, "Equivalence of Hybrid Dynamical Models," *Automatica*, vol. 37, no. 7, pp. 1085-1091, 2001.
- [12] M. S. Ghasemi, and A. A. Afzalian, "Robust Tube-based MPC of Constrained Piecewise Affine Systems with Bounded Additive Disturbances," *Nonlinear Analysis: Hybrid Systems*, vol. 26, pp. 86-100, 2017.
- [13] B. Pregelj, and S. Gerki, "Hybrid Explicit Model Predictive Control of a Nonlinear Process Approximated with a Piecewise Affine Model," *Journal of Process Control*, vol. 20, no. 7, pp. 832-839, 2010.
- [14] D. Q. Mayne, and S. Raković, "Optimal Control of Constrained Piecewise Affine Discrete-time Systems," *Computational Optimization & Applications*, vol. 25, no. 1-3, pp. 167-191, 2003.
- [15] C. Y. Lai, C. Xiang, and H. L. Tong, "Data-based Identification and Control of Nonlinear Systems via Piecewise Affine Approximation," *IEEE Transactions on Neural Networks*, vol. 22, no. 12, pp. 2189-2200, 2011.
- [16] D. W. Clarke, C. Mohtadi, and P. S. Tuffs, "Generalized Predictive Control-Part 1. The Basic Algorithm," *Automatica*, vol. 23, no. 2, pp. 137-148, 1987.
- [17] O. A. Felipe, G. B. Didier, and G. Eduardo, "Sliding Mode Control Applied to MIMO Systems," *Engineering Letters*, vol. 27, no. 4, pp. 802-806, 2019.
- [18] B. C. Ding, "Robust Model Predictive Control for Multiple Time Delay Systems with Polytopic Uncertainty Description," *International Journal of Control*, vol. 83, no. 9, pp. 1844-1857, 2010.
- [19] E. Kayacan, E. Kayacan, H. Ramon, and W. Saeys, "Distributed Nonlinear Model Predictive Control of an Autonomous Tractor-Trailer System," *Mechatronics*, vol. 24, no. 8, pp. 926-933, 2014.
- [20] H. Li, Y. Shi, and W. Yan, "On Neighbor Information Utilization in Distributed Receding Horizon Control for Consensus-Seeking," *IEEE Transactions on Cybernetics*, vol. 46, no. 9, pp. 2019-2027, 2016.
- [21] M. Farina, and R. Scattolini, "Distributed Predictive Control: A Non-cooperative Algorithm with Neighbor-to-neighbor Communication for Linear Systems," *Automatica*, vol. 48, no. 6, pp. 1088-1096, 2012.
- [22] J. Zhan, Z. P. Jiang, Y. Wang, and X. Li, "Distributed Model Predictive Consensus with Self-triggered Mechanism in General Linear Multi-agent Systems," *IEEE Transactions on Industrial Informatics*, vol. 15, no. 7, pp. 3987-3997, 2019.
- [23] S. Shamaghdari, and M. Haeri, "Model Predictive Control of Nonlinear Discrete Time Systems with Guaranteed Stability," *Asian Journal of Control*, vol. 22, no. 2, pp. 657-666, 2020.
- [24] Rohit Kawathekar, and James B. Riggs, "Nonlinear Model Predictive Control of a Reactive Distillation Column," *Control Engineering Practice*, vol. 15, no. 2, pp. 231-239, 2007.
- [25] Y. Hu, J. Sun, S. Z. Chen, X. Zhang, and D. Zhang, "Optimal Control of Tension and Thickness for Tandem Cold Rolling Process Based on Receding Horizon Control," *Ironmaking & Steelmaking*, no. 5, pp. 1-11, 2019.
- [26] C. Ren, X. Li, X. Yang, and S. Ma, "Extended State Observer Based Sliding Mode Control of an Omnidirectional Mobile Robot with Friction Compensation," *IEEE Transactions on Industrial Electronics*, vol. 66, no. 12, pp. 9480 - 9489, 2019.
- [27] M. Amanullah, C. Grossmann, M. Mazzotti, M. Morari, and M. Morbidelli, "Experimental Implementation of Automatic 'Cycle to Cycle' Control of a Chiral Simulated Moving Bed Separation," *Journal of Chromatography A*, vol. 1165, no. 1-2, pp. 100-108, 2007.
- [28] A. Rajendran, G. Paredes, and M. Mazzotti, "Simulated Moving Bed Chromatography for the Separation of Enantiomers," *Journal of Chromatography A*, vol. 1216, no. 4, pp. 709-738, 2009.

Song Li is a postgraduate student in the School of Electronic and Information Engineering, University of Science and Technology Liaoning, Anshan, 114051, PR China. His main research interest is modeling and control methods of complex industrial process.

Dong Wei is with the School of Electronic and Information Engineering, University of Science and Technology Liaoning, Anshan, 114051, PR China. His main research interest is modeling and intelligent control of complex industry process.

Jie-Sheng Wang received his B. Sc. and M. Sc. degrees in control science from University of Science and Technology Liaoning, China in 1999 and 2002, respectively, and his Ph. D. degree in control science from Dalian University of Technology, China in 2006. He is currently a professor and Doctor's Supervisor in School of Electronic and Information Engineering, University of Science and Technology Liaoning. His main research interest is modeling of complex industry process, intelligent control and Computer integrated manufacturing.

Zhen Yan is a postgraduate student in the School of Electronic and Information Engineering, University of Science and Technology Liaoning, Anshan, 114051, PR China.

Shao-Yan Wang is a professor and Doctor's supervisor in School of Chemical Engineering, University of Science and Technology Liaoning, Anshan, 114051, P. R. China.